CHAPTER - 6

GEOCHEMISTRY

6.1 Introduction

The word geochemistry is constituted from two words; geo (the Earth) and chemistry (branch of science deals with chemical transformation). To understand and quantify the chemical composition, structural property of rocks, a petrologist needs to look for the chemistry of the rock termed as geochemistry. The earth crust has dominantly been made up of primary rock derived from a magma called igneous rocks. The nature of metamorphic rock suits can be broadly defined by major and trace element chemistry. Silicates are the fundamental unit for most metamorphic rocks formed from aggregates of one or more minerals, naturally occurring inorganic chemical compounds.

The present chapter embodies the geochemical attributes of the mafic granulites and pelitic granulites within the designated area of investigation. It provides a hypothesized model for these rocks' evolutionary history. Geochemical characterization of metamorphic rocks is an essential feature to know petrological evolution of the rocks of the study area. The purpose of the present study is:

(i) Whether the granulites are magmatic/ orthometamorphic or parametamorphic,

(ii) Whether magmatic signatures have been preserved and if so what was the nature of source magma or tectonic environment for magma generation,

(iii) Whether there is an overall signature of depletion of large-ion lithophile element (LILE) and an enhancement of K/Rb ratios, and

(iv) To what extent different granulites are chemically comparable to the Indian granulites province's similar suites.

6.2 Major oxides Geochemistry

In metamorphic rocks, the oxides that are most prevalent are arranged in ascending order based on their atomic numbers. These oxides include sodium oxide (Na_2O), magnesium oxide (MgO), aluminium oxide (Al_2O_3), silicon dioxide (SiO_2), phosphorus pentoxide (P_2O_5), potassium oxide (K_2O), calcium oxide (CaO), titanium dioxide (TiO_2), manganese oxide (MnO), and iron oxide (Fe, encompassing both ferric Fe_2O_3 and ferrous FeO). These tools are mostly utilised for the purposes of rock categorization and the construction of variation diagrams. The Earth's crust contains significant elements that are present in quantities exceeding 1 wt %, whereas trace elements are found in quantities less than 1 wt %. This distinction is made due to the fact that the behaviour of major oxides in magmas may be observed and analysed using differentiation indices. Similarly, trace elements exhibit analogous behaviour to major elements due to their ability to replace major elements. Therefore, geochemistry serves as a highly efficient method for distinguishing the protolith of metamorphic rocks, determining the underlying magmatic processes, characterising the properties of melt, and assessing the tectonothermal conditions through quantitative measurements and analysis of geochemical patterns. The determination of the protoliths' origin, whether sedimentary or igneous, for metamorphic rocks is a subject of great interest. Numerous discrimination diagrams have been utilised in scholarly literature to aid in this process. All mafic granulites exhibit positive differentiation factor (DF) values, indicating that the origins of these granulites can be traced back to igneous processes [329].

6.3 Trace Element Geochemistry

Trace element geochemistry has been appreciated for establishing or determining the Earth's evolution, and also used for recognizing their depositional environment. The comparative abundances of trace elements are broadly recognized for the evolutionary process because they are sensitive to partial melting, crystal fractionation and source composition. The trace element proportion of the melt depends on the parent material, the melting process, the remaining crystal phases after removing the melt, any differentiation before to complete crystallization and any possible interaction with rocks, melts or fluids [185]. The trace elements would provide better tools for understanding the geochemical process than the major oxides. The concentration of these elements (Rb, Sr, Nb, Zr, Ba, Cs, Hf, Ta, Pb, etc.) in rock is less than 0.1% and are expressed in parts per million (ppm), they are used to study elemental distribution in crystal-melt equilibria. Trace elements that have priority in the mineral phase are described as compatible. In contrast, elements that have a melting preference are said to be incompatible [330], based on the charge-size ratio or ionic potential, incompatible elements are categorized into high field strength (HFS) element (Sc, Ta, Y, U, Nb, Pb, Hf) and LILE (Cs, Rb, Ba).

6.4 Rare Earth Elements Geochemistry

The geochemical behaviour of Rare Earth Elements (REE) changes gradually from La to Lu. REE contents of igneous rocks offer significant evidence about the magma source, the degree of partial melting of that source, the degree of crustal contamination, and the quantity of crystal fractionation during magma evolution. REE are normally deliberated to be immobile when post igneous alteration and low-grade metamorphism [185].

REE patterns are valuable tools for comprehending the petrogenesis process of magmatic entities and discerning their tectonic context [331]. The rare earth elements (REE) consist of a collection of 15 trace elements, ranging in atomic number from 57 (Lanthanum) to 71 (Lutetium). Among these elements, 14 occur naturally, with the exception of Promethium (Pm). To enhance convenience, the rare earth elements (REEs) are categorised into two distinct sub-groups: (i) The elements from La to Sm are commonly referred to as the light rare earth elements (LREE), while (ii) the elements from Gd to Lu are acknowledged as the heavy rare earth elements (HREE). However, the utilisation of middle rare earth elements (MREE) encompasses the elements ranging from Samarium (Sm) to Holmium (Ho) [332]. In the natural environment, the majority of rare earth elements have a 3+ oxidation state, sometimes referred to as trivalent. However, it is worth noting that Ce4+ is an exception as it is typically found in an oxidised state, while Eu2+ is an exception as it is commonly found in a reduced state under typical geological settings.

6.5 Analytical techniques

In the present study, 21 representative samples from adjoining areas of Betul of the Central Indian Tectonic Zone (CITZ) were chemically analysed for the major, trace and REEs. The geochemical data of various rocks are given in Tables 6.1-2. To avoid alteration rind, samples were gathered from the fresh surface in a manner that ensured their representativeness, then powdered using a jaw crusher, pulverization mill and agate mortar. XRF carried out whole-rock major elemental analyses, and trace, REE analysis were carried out by ICP-MS, the details of which are given below. To understand the behaviour of major, trace and REEs in different rocks by varieties of diagrams, ratios correlations have been used.

6.5.1 XRF and ICP-MS

X-ray Fluorescence (XRF) and Inductive Coupled Plasma-Mass Spectrometry (ICP-MS) techniques were employed to conduct analyses on main oxide, trace, and Rare Earth Element (REE) compositions. The aforementioned research activities were conducted at the Birbal Sahni Institute of Palaeosciences (BSIP) located in Lucknow, India. The samples were prepared using the pressed powder method, where boric acid was used as a binder at a ratio of 2:3 (boric acid to sample). The examination of the principal oxides was conducted through the utilisation of X-ray fluorescence (XRF) analysis. This analysis was performed utilising a wavelength dispersive XRF machine known as AXIOS MAX. The machine operated at a power of 4KW and possessed an analytical range spanning from 60kV to 160mA. The specimens were manufactured by compressing powder into pellets using a 'kameyo' machine with a pressure range of 15-20 tonnes, yielding pellets with a uniform thickness of 4mm. Rare earth elements (REEs) were subjected to analysis using inductively coupled plasma mass spectrometry (ICP-MS). The ICP-MS instrument utilised for this analysis was an Agilent model, specifically the ICP-MS 7700. All solutions were made using ultrapure water with a conductivity of 18.2 MX. The samples underwent digestion by utilising a 30 mg (300 mesh) sediment powder, which was treated with supra pure acid (HF, HClO4, HNO3). Four solutions with concentrations of 10, 40, 100, 200, and 300 parts per billion (ppb) for all elements were generated using 71A and 71B multi-element calibration standard solutions from Inorganic Ventures. These solutions were utilised as external calibration standards. The data set is expected to have an error rate of less than 5% when the appropriate calibration curve is applied.

6.6 Mafic granulite

6.6.1 Major oxides

The compositional variation of the major oxides of the mafic granulites are given; SiO_2 (46.76–52.66 wt%), Al_2O_3 (13.43–18.21 wt%), MgO (4.68–12.08 wt%), Fe_2O_3 (13.54–17.89 wt%), K_2O (0.45–1.29 wt%), TiO_2 (0.14–1.71 wt%), CaO (7.57–9.26 wt%), Na_2O (1.93–2.54 wt%) and P_2O_5 (0.10–0.56 wt%). The analytical data shows that all the mafic granulites are olivine normative with 47 to 50 wt% in silica. The mafic granulite samples show basaltic nature when plotted on the total alkalis vs silica (TAS) plot [182] (Fig.6.1a). Where silica content is between 45–50 wt%, and combined alkali (K_2O + Na_2O) is less than 5%, which corresponds to basalt. The Bivariate diagrams (Fig.6.2) plotted for the major oxides of mafic granulites. Major oxides are plotted against the MgO wt% to reveal magmatic evolution through elemental partitioning. A negative correlation is found between MgO with Fe_2O_3, MnO, and TiO_2, while a positive correlation between MgO with SiO_2, Al_2O_3, and CaO is experienced. During post crystallization processes, high mobility elements represent scattered data plots of MgO with Na_2O and K_2O. The decrease in Fe_2O_3 and TiO_2 with increasing MgO with the robust negative anomaly of Nb, and Ti, recommends fractionation of Fe-Ti oxides for all the mafic granulite samples.

6.6.2 Trace elements

Trace element data provide valuable information on the rocks' pre-metamorphic parentage because many elements, especially the rare earth element (REE), are believed to be unaffected by regional metamorphism unless partial melting is involved [334]. However, some elements such as Ba, Rb, Sr and LREE are mobile and are not believed to be useful for tectono-magmatic discrimination purpose, therefore, elements such as

Ti, Cr, Ni, Fe, Nb, Ta, Zr, Hf, and V, which are comparatively immobile during weathering and metamorphism is used as far as possible. The PM normalized trace elements of the mafic granulites show a negative peak for Ti, Nb, Sr and positive peak for U, Ta which reveals a rich LILE pattern High elemental concentrations of Mg, V, and Co suggest that they be derived from primary magmatic sources [335]. The amount of HFSE (Y, U, Pb, Hf, Nb, Ta) is small, indicating that the rock is derived from the mafic source. Nb has negative anomalies that showed crustal contamination. Besides, mafic granulites have modest Cr, Ni content, and Ni values between 18.06 ppm and 469 ppm and HFSE (high field strength element) ratios as, Nb/Y less than 0.5.

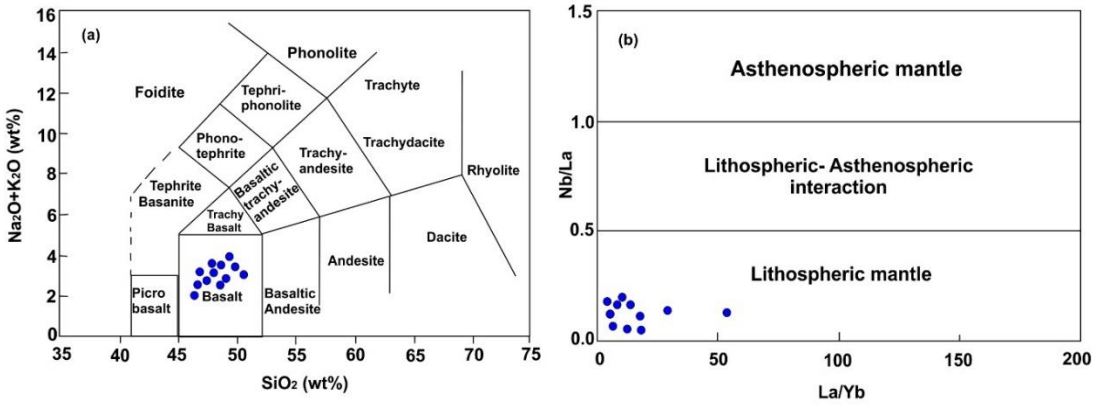

Figure 6.1(a) The chemical classification and nomenclature of volcanic rocks using total alkalis versus silica diagram of mafic granulite (after [182]), (b) La/Yb vs. Nb/La plot (after [333]) ruling out significant Lithospheric contribution in the mantle source region of the mafic granulites of Betul Belt (BB).

Since the element-element ratios are important in the petrogenesis of magmatic rocks. Notably, K/Rb ratios of the present rocks range from 178 to 873, so the average crustal value is over 250. The Yb-Th discriminant diagram (Fig.6.4a) of mafic granulite shows the calc-alkaline nature [184]. Y-La-Nb discrimination diagram of mafic granulites suggests an orogenic tectonic setting (**Fig.6.4b**) [336].

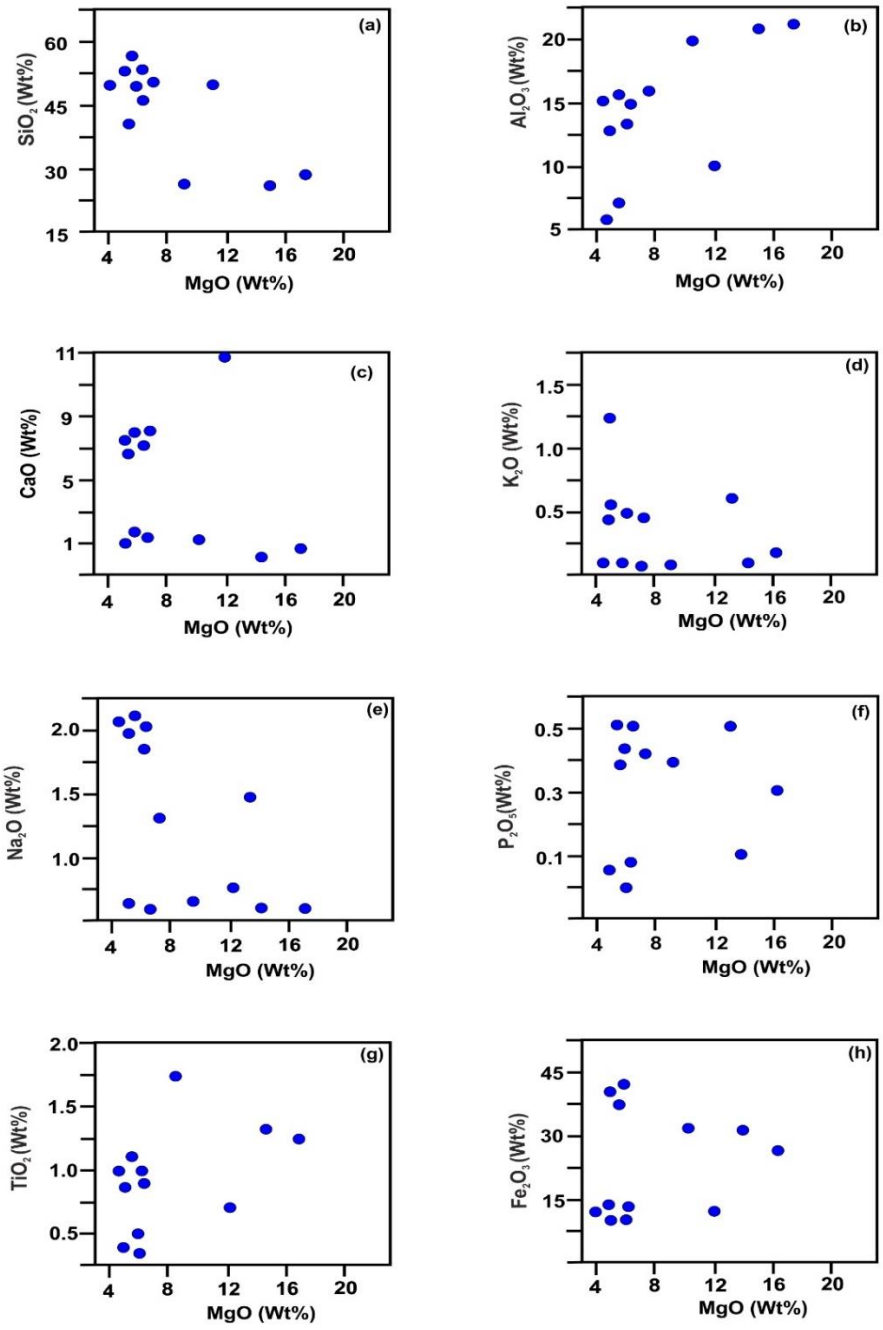

Figure 6.2 Bi-variate plots (oxides in wt%) (a) MgO vs SiO_2, (b) MgO vs Al_2O_3, (c) MgO vs CaO, (d) MgO vs K_2O (e) MgO vs Na_2O, (f) MgO vs P_2O_5, (g) MgO vs TiO_2, and (h) MgO vs Fe_2O_3 for the mafic granulites of Betul Belt (BB) are showing good fractionation trends except for K_2O and Na_2O.

6.6.3 REEs

REE concentrations are generally normalized to an authentic reference standard, mostly chondritic meteorites' values. Chondritic meteorites were selected as they are

considered relatively unfractionated solar system samples dating back to the original nucleosynthesis. To compare graphically, REEs are represented by the spider diagram for the mafic granulites (Fig.6.3b). The Eu anomaly ratio is a measure of [206] and a value more than 1.0 indicates a positive anomaly while a value of lesser than 1.0 is a negative anomaly. The Eu anomalies can be determined by comparing analysed concentration with a probable concentration projected between the normalized values of Sm and Gd (EuN*). The variation of Eu_N/Eu_N* is also limited (0.18 to 0.57), suggesting a source signature rather than feldspar fractionation [338].

The REE distribution patterns (Fig.6.3b) of mafic granulites from Betul Belt show that the rocks are slightly enriched in the LREE than HREE and show negative Eu anomaly. The negative Eu anomalies detected may be due to eliminating plagioclase from a melt whereas the positive Eu anomalies may be due to the enrichment of plagioclase in the melt showing low fractionation in the rocks. The basalts' sub-parallel REE patterns suggest that compositional variation resulted from crystal fractionation. [39]. The $(La/Yb)_N$ ratios exhibit a range of fractionation degrees, spanning from 0.40 to 2.18, which can be considered relatively low for the rocks under investigation.

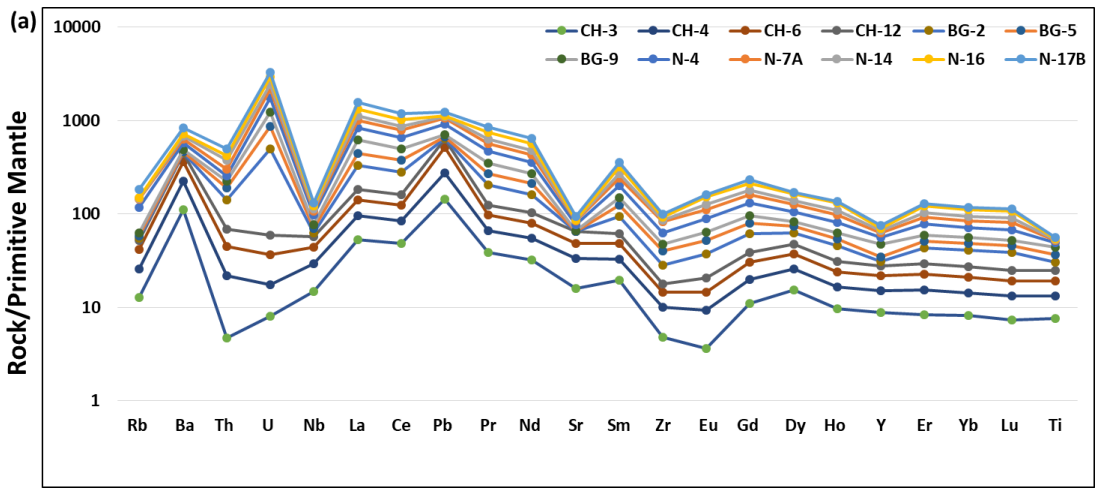

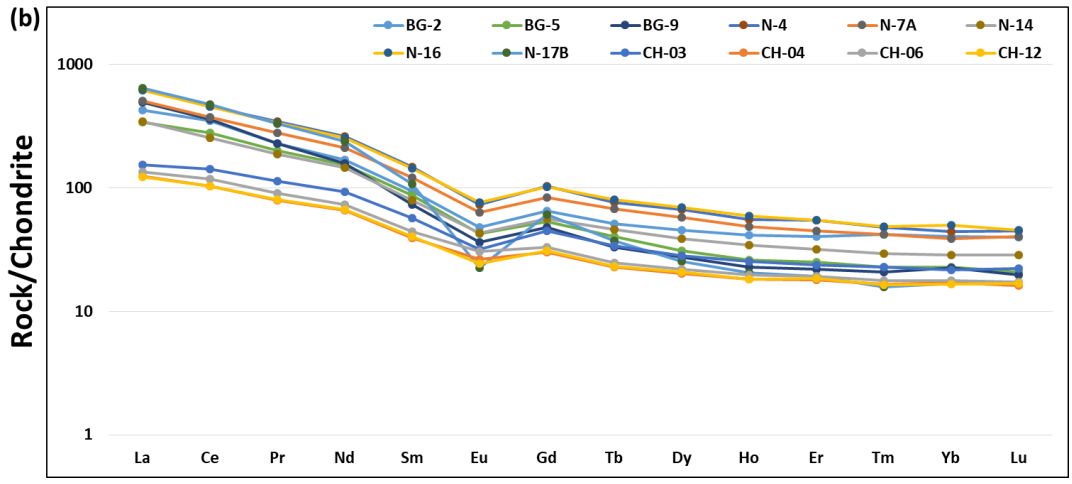

Figure 6.3(a) Primitive mantle [337] normalized multi-element spider diagram for the mafic granulites of Betul Belt and (b) Chondrite normalized [337] rare earth element distribution pattern.

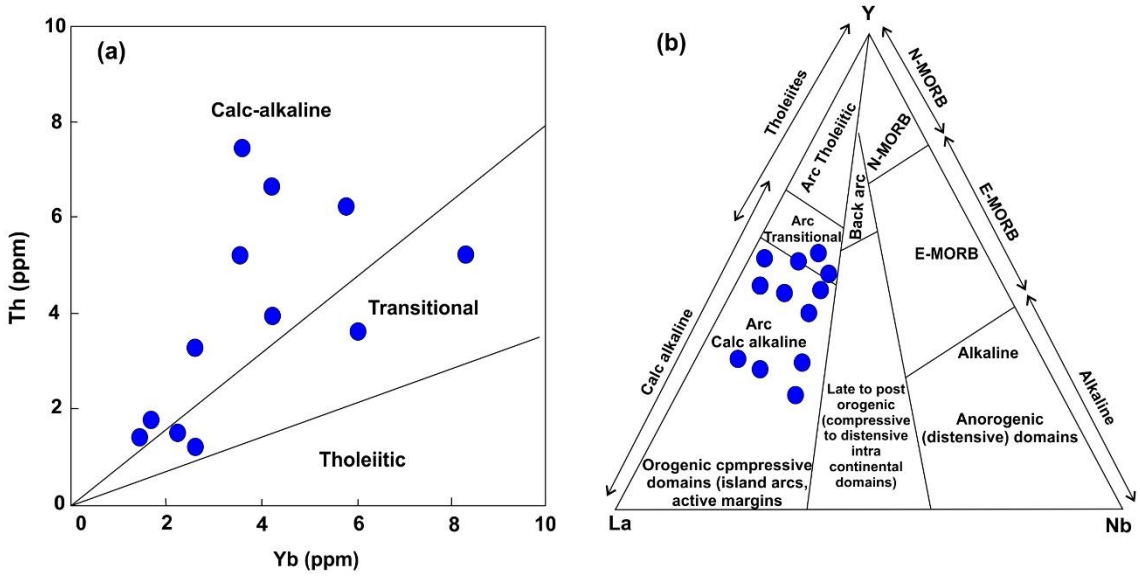

Figure 6.4 Tectonic discrimination diagrams for Betul mafic granulites; (a) Th vs Yb bivariant plot (after [184]), (b) Y-La-Nb ternary diagram (after [336]) illustrating orogenic affinity, and both diagram show all the samples belong to Calc-alkaline nature of basalt.

6.6.4 Discussion

Several important issues of Betul mafic granulites are discussed based on the current geochemical studies. This discussion is mafically centered on the premetamorphic signature of the mafic granulites, nature and differentiation trend of

magma, and tectonic environment. One of the important issues relates to granulite facies metamorphism, i.e., the selective depletion of the mafic granulites during granulite facies metamorphism is also addressed. From the present geochemical study, it is clear that the precursor rocks of the mafic granulites were of magmatic origin; the documentary evidence supporting this view is the positive DF values derived by [329].

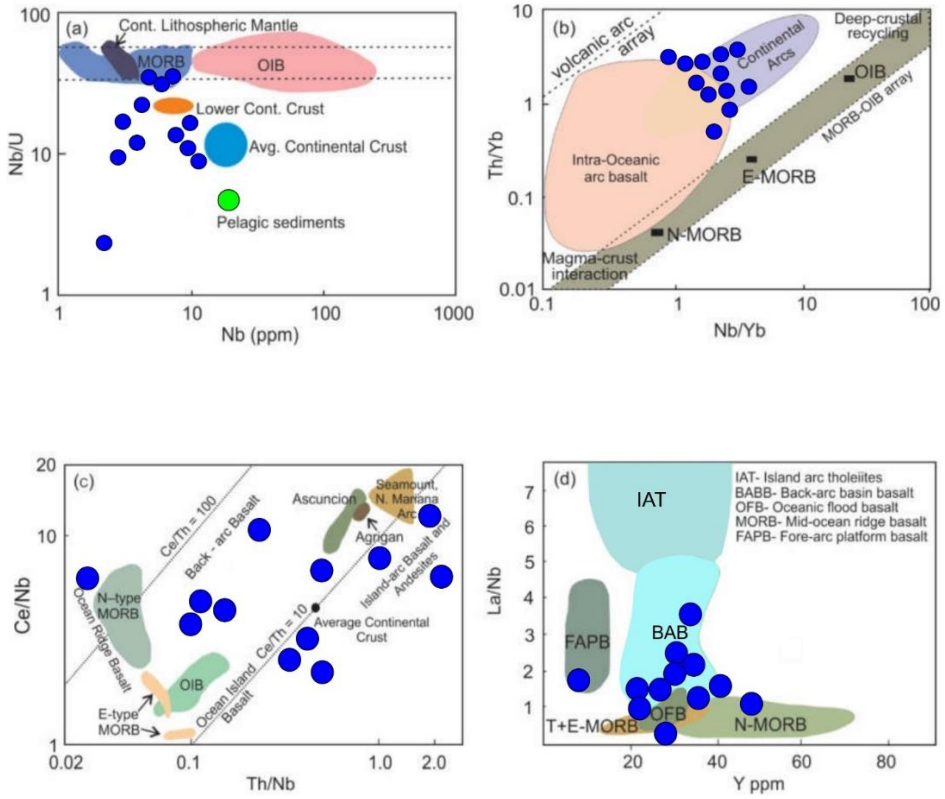

Figure 6.5(a) Nb (ppm) vs Nb/U plot ([340] and references therein), (b) Th/Yb vs Nb/Yb diagram [341] depicting a subduction-related enrichment for the Betul mafic granulites samples. Fields for intraoceanic arc basalt is from [342] and reference therein. (c) Th/Nb vs Ce/Nb (after [343], and (d) Y vs La/Nb diagram (after [344], N-MORB: normal mid-ocean ridge basalt. E-MORB: enriched mid-ocean ridge basalt. OIB: ocean island basalt.

6.6.4.1 Petrogenesis

Geochemical composition of sedimentary/metasedimentary rocks plays a crucial role as a sensitive indicator in determining their provenance and to constrain the

tectonic setting in which they were deposited, and also to understand the evolutionary development of the early continental crust [195-198, 200, 201, 203-205, 339].

6.6.4.1.a Implications from trace and REEs

The nature of the trace element and the REE pattern progressively suggests protoliths' origin from the magma fractionation [186]. The chondrite-normalized REE patterns of mafic granulites are showing low fractionated REE patterns, and are rich in LREE and relatively low HREE with a negative Eu anomaly (Fig.6.3b). These characteristics may be recognized as the parent rock has plagioclase-rich and garnet free composition. On the Harker diagram, CaO-MgO (Fig.6.2) co-variation requires plagioclase ± clinopyroxene precipitation from the mafic liquid. Mantle peridotite represents the preferred accommodation of LREE in clinopyroxene while HREE within the garnet [188]. The higher abundances of Rb, Ba, U, Pb and LREE in mafic granulites are interpreted as a result of a rich component of the fluid [191]. Th, U, and Pb exist as high concentrations within the basaltic protolith, indicating crustal components' involvement at their origin. Nb and Ti are a negative anomaly and are observed to be characteristics of the subduction-related environment. The relative abundance of REE in igneous and metamorphic rocks is generally considered a useful indicator of tectonomagmatic affinity. The characteristic flat to depleted REE content as reflected from the present samples are assumed to be the melt from the primitive mantle with little or no enrichment to deplete the LREE relative to the HREE.

6.6.4.1.b Mantle source and subduction zone enrichment

It is known that the present mafic granulites are predominantly tholeiitic with olivine normative and thus suggest one of their mantle sources underwent shallow and hydrous melting. This mantle-derived magma's crustal contamination is one of the

crucial issues for mafic granulites. Several geochemical parameters can be used to evaluate the problem of mafic magma contamination by continental crust, and the following is a discussion of their application to this magma composition of rocks. Intermediate composition of SiO_2 (<49 wt %) with a low U (0.20–2.12 ppm), Th (0.40–6.21 ppm) and Pb (1.05–17.33 ppm) suggests that magma arises from bulk-assimilation of continental crust. Th/La ratio (>0.12) indicates potential crustal contamination during the emplacement of mafic magma [337]. The negative anomaly of HFSE is demarcated as subduction-related magmatism, and it also supports HFSE elements present in the Ti bearing remaining phases within mantle-derived magma. Mantle-derived magma is also identified by the HFSE/LREE proxy [333] and Nb/La (< 0.37) ratio, which is lower for the basaltic protolith and represents the provenance of the lithospheric mantle (Fig.6.1b). The Nb/U versus Nb discrimination diagram [340] for the mafic granulites is lower than the MORB and OIB (Nb/U ~ 25), which refers to the melt phase originating from the subducted slab and being metasomatized from the mantle source (Fig.6.5a). The subduction influenced source is also sustained by high Th/Yb and low Nb/Yb content; these rock data are beyond the MORB-OIB array in field of intra-oceanic arc basalt (Fig.6.5b). High Th/Yb and low Nb/Yb values have indicated that basaltic magma was a subducted-slab product derived from the mantle source (Fig.6.5b).

6.7 Pelitic granulite

The current state of the pelitic granulites in the given region has been tested by calculating their values according to DF [329], and they are found to be pure of sedimentary origin. These rocks have SiO_2 from 60.80 wt% to 65.49 wt%, highly variable Al_2O_3 contents (11.23 wt% to 18.21 wt%) and relatively low FeO contents and

higher values of K_2O as in mafic granulites due to crustal predominance of protoliths. The FeO/FeO+ MgO ratio is between 0.81 and 0.97.

6.7.1 Whole-rock geochemistry

A total of seven pelitic granulite samples (3 from Sonaghati and 4 from Biskhan) have been analysed. The LOI-contain (Loss of ignition) ranges from 1.15 to 3.74. SiO_2 composition exhibits a wide variation (60.80-65.49 wt%), the total alkali-silica (TAS, [345]) diagrams (Fig.6.7a and b) of pelitic granulites are compositionally diorite and monzonite. In contrast, few samples are gabbroic; the pelitic granulite protolith was formed from various sedimentary provenances. All samples have a ferroan character (Fig.6.7), and most samples are peraluminous with one sample is metaluminous (A/CNK= 0.88-1.39) (Fig.6.7c). However, these are calc alkalic to alkali-calcic variable composition, but a sample has the calcic composition (Fig.6.7d). Na_2O vs K_2O diagram (Fig.6.7e) represents shoshonitic and ultra-potassic composition, but the SiO_2 vs K_2O diagram (Fig.6.7f) clarifies that all the samples are of shoshonitic nature.

6.7.2 Trace and rare earth element patterns

The trace element spider-diagram with normalization of the primitive mantle of pelitic granulites defines positive anomaly for Ba, Th, Pb, Nd, Hf, Sm and Y whereas LILE (Rb, Sr) and HFSE (Nb, Ti) has negative anomaly (Fig.6.8a and b). All the samples represent negative Eu anomalies, and no positive anomalies are observed (Fig.6.8b). The negative anomalies can attributed to the low fractionation of plagioclase in mineral phase and more concentration of plagioclase in the melt phase.

6.7.3 Discussion

The geochemical data of pelitic granulites show their unusual composition because they do not correspond to any normal igneous or sedimentary rocks. The mineral of the pelitic granulites total composition suggests that they were derived from argillaceous parent rocks.

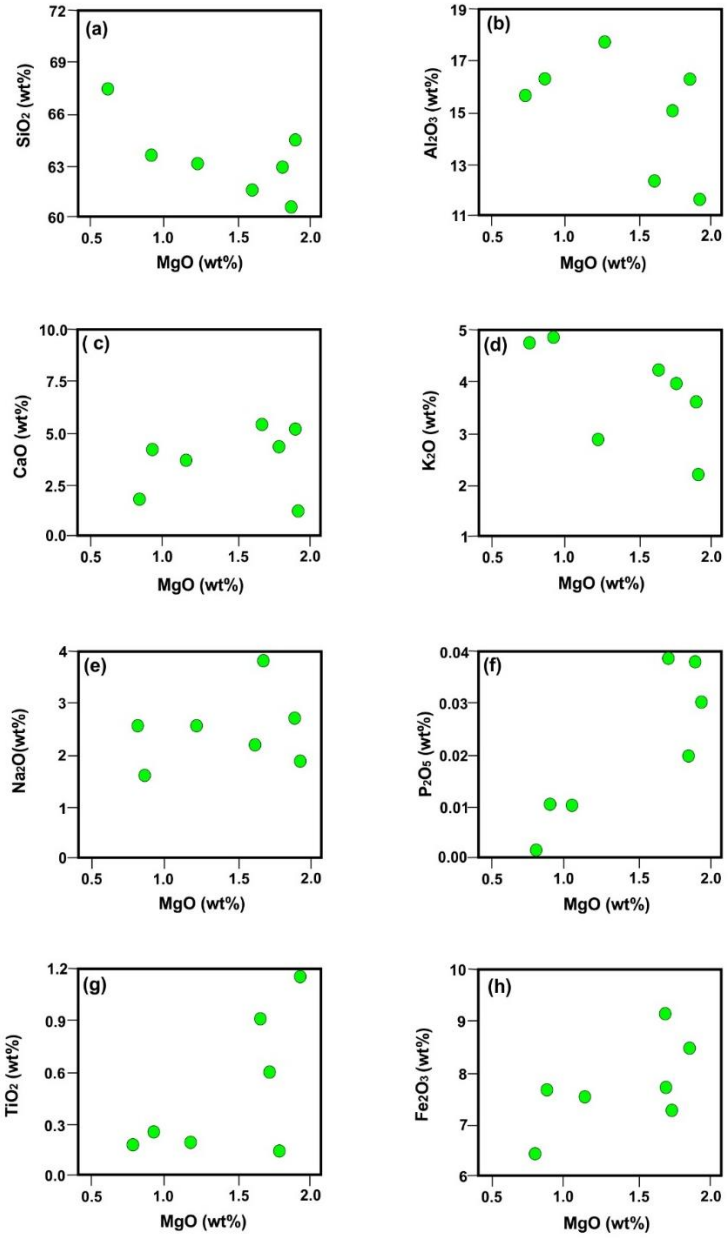

Figure 6.6 Bi-variate plots (oxides in wt%) (a) MgO vs SiO_2, (b) MgO vs Al_2O_3, (c) MgO vs CaO, (d) MgO vs K_2O (e) MgO vs Na_2O, (f) MgO vs P_2O_5, (g) MgO vs TiO_2, and (h) MgO vs Fe_2O_3 for the pelitic granulites of Betul Belt (BB) are showing good fractionation trends except for K_2O and Na_2O.

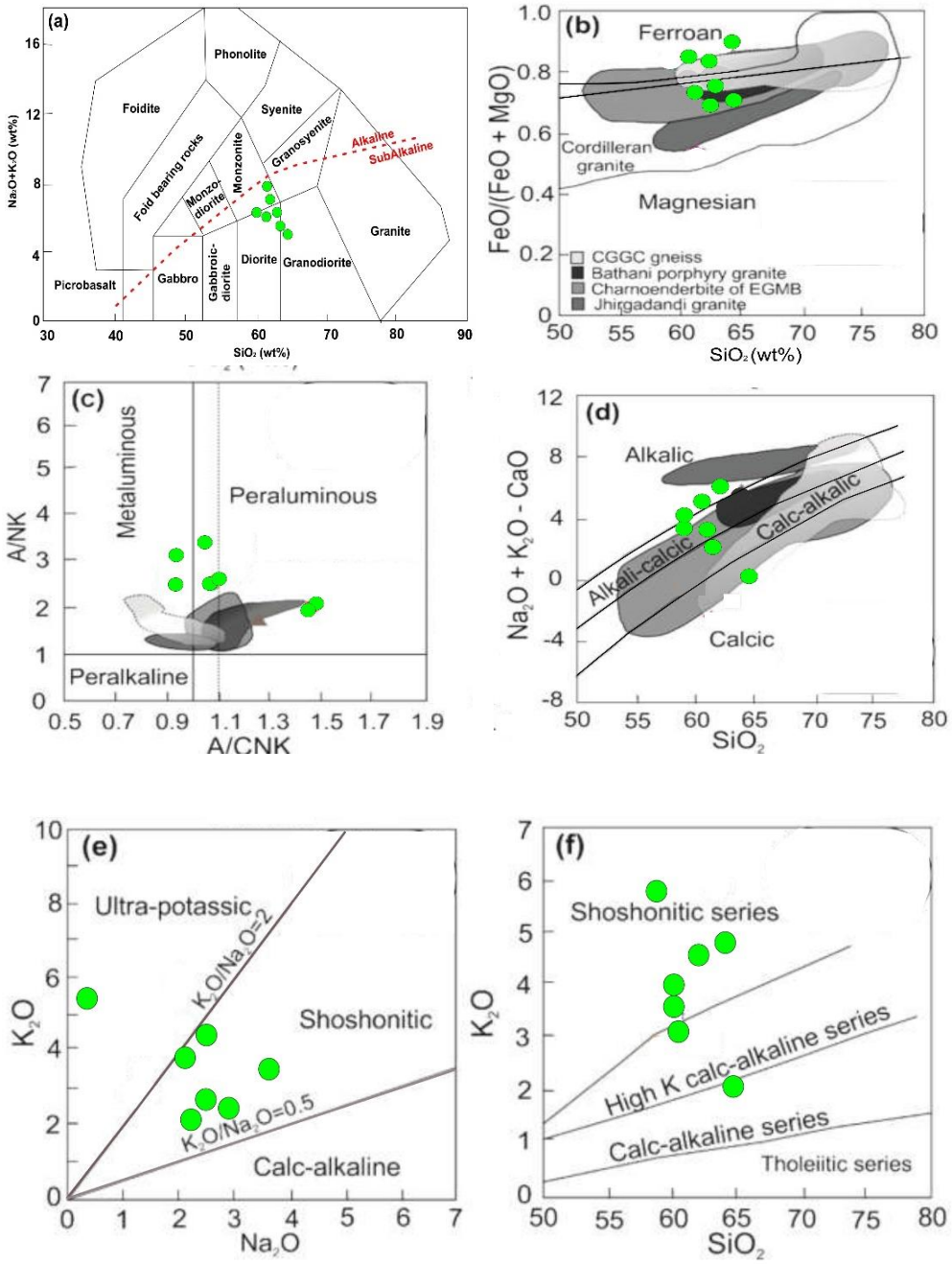

Figure 6.7(a) Total alkali silica diagram after Middlemost (1994). (b-c) Granitoid classification scheme by [349] revealing (b) magnesian to ferroan, (c) slightly peraluminous nature of the studied rock (d) calcalkalic to alkali-calcic. Field of the Cordilleran granites is plotted after [349]. The data also compared with Bathani porphyritic granite [253], Charno-enderbite of Eastern Ghats Mobile Belt [350], Jhirgadandi Granite [26], Augen gneiss of Dumka from CGGC [266]. (e) Na_2O vs K_2O diagram (after [351]; (f) K_2O vs SiO_2 plot after [352] showing the shoshonitic nature of the rock.

However, no undesirable sedimentary structures have survived due to the rocks recrystallization and reconstitution. Generally, the element's movement is reported between the coexisting mineral phases, so few elements tend to migrate from the crystal phase to the melt phase during metamorphism. Pelitic granulites contain a good amount

of Ba and Rb, as the feldspar is an essential mineral for hosting Ba and Rb in terrigenous sedimentary rocks. Moreover, the analysed geochemical data indicate that pelitic granulites are probably redeposit, and metamorphosed products of Paleoproterozoic weathered crusts.

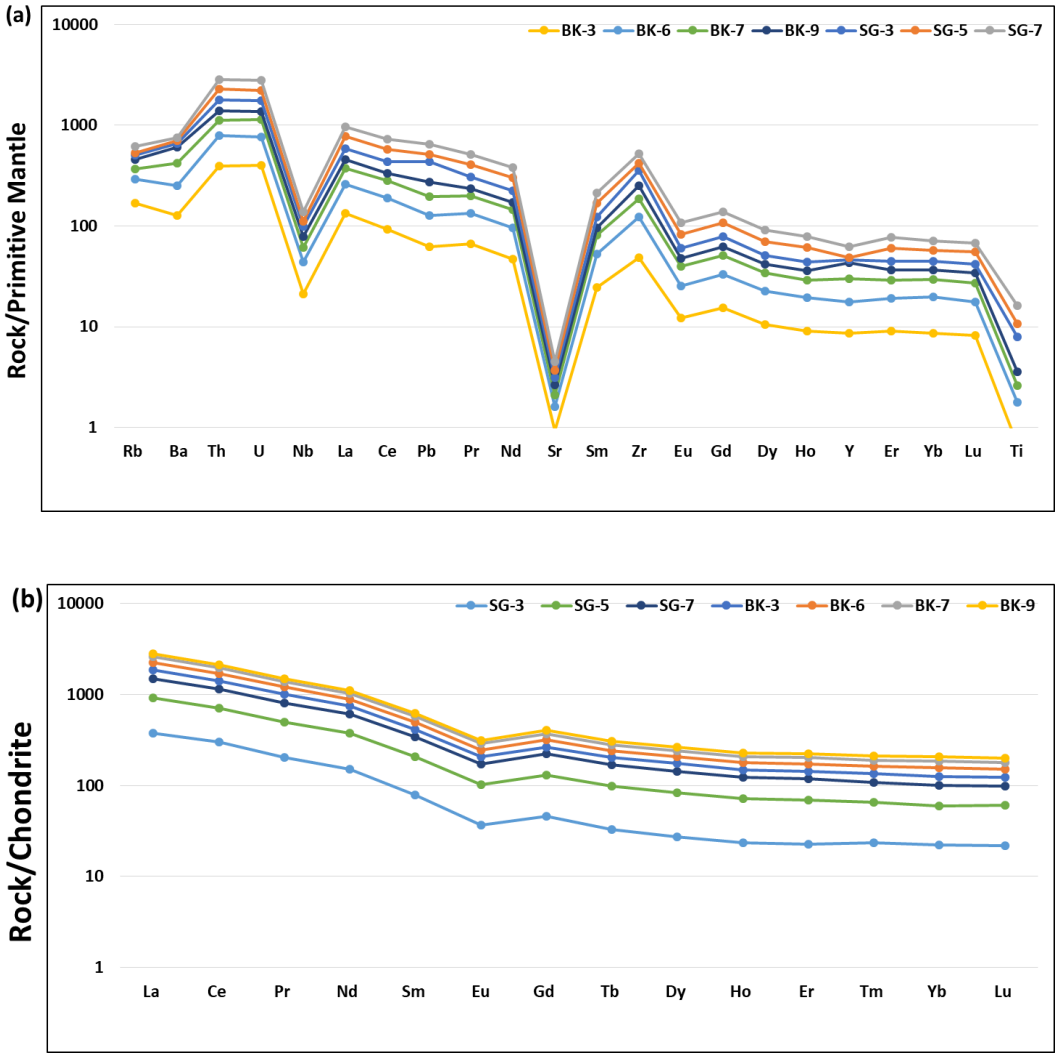

Figure 6.8(a) Primitive mantle normalized multi-elements spider diagram of pelitic granulite after [337]. (b) Chondrite normalized REE plot after [337] showing uniform and nearly smooth REE pattern.

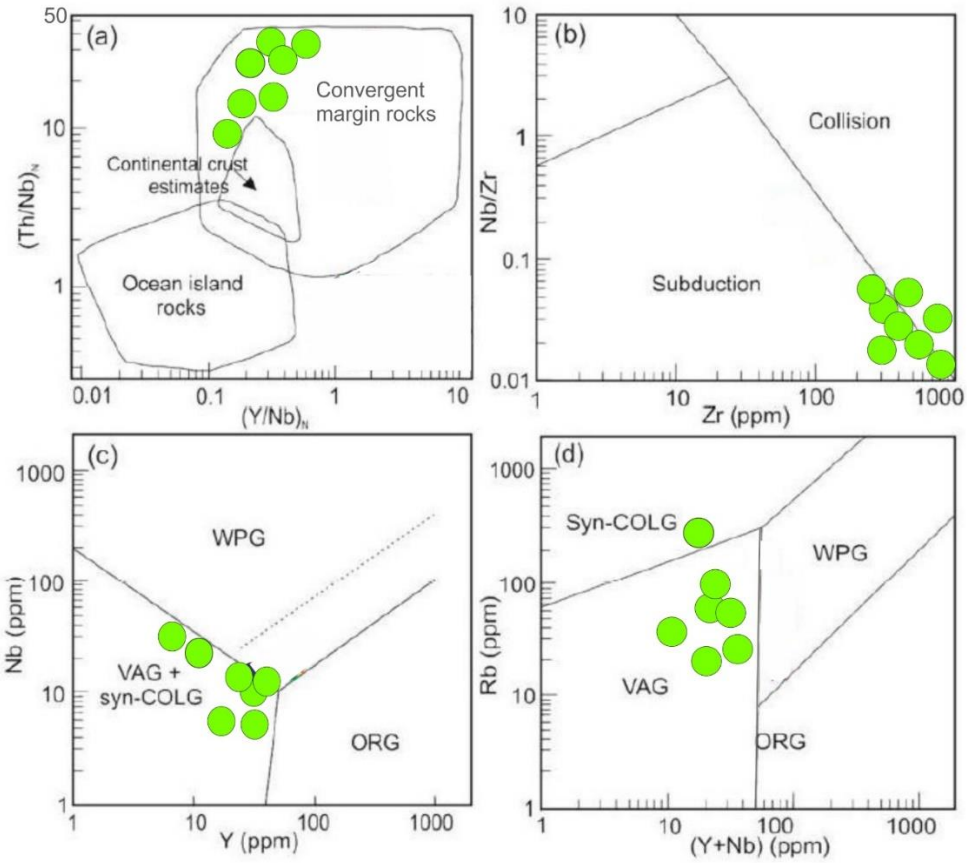

Figure 6.9. (a) (Y/Nb)N vs (Th/Nb)N [346] used to discriminate tectonic regimes of pelitic granulites from the Betul Belt. (b) Zr vs Nb/Zr plot with fields from [347] showing subduction tectonic regime for the genesis of protolith of pelitic granulites, (c) Y vs Nb tectonic discrimination diagram (after [348] plotted with pelitic granulites mostly showing an affinity towards the within-plate granite (WPG). (d) Y+Nb vs Rb tectonic discrimination diagram plotted for pelitic granulite. Syn COLG: syn-collisional granite; WPG: within plate granite; VAG: volcanic arc granite; ORG: ocean ridge granite [348].

6.7.3.1 Tectonic implications

Upon establishing the correlation between the $(Y/Nb)_N$ against $(Th/Nb)_N$ diagram [346], it has been employed to discern between oceanic islands, continental crust, and rocks from convergent margins. Notably, all examined samples are situated within the field corresponding to convergent margin rocks (Fig. 6.9a). The figure depicting the Zr against Nb/Zr relationship (Figure 6.9b) offers empirical support for the hypothesis that the precursor rock of pelitic granulites underwent geological

processes linked to subduction. [347]. The Y vs Nb and Rb vs (Y+Nb) tectonic discrimination diagram shows that the protolith has an affinity towards the VAG+Syn-COLG (Fig.6.9c and 6.9d) [348]. The Gaya region of Mahakoshal Mobile Belt (MMB) demarcates tectonic affinity similar to the within-plate granite setting (Fig.6.9c,d) and continental margin magmatic rocks (fig.6.9a) for pelitic granulites [4,353]. The spider diagram displayed a positive anomaly in Pb and a negative anomaly in Nb, indicating that the pelitic granulites' protolith formed within a collisional tectonic environment. The observed increase in concentrations of potassium (K), thorium (Th), uranium (U), lead (Pb), and the sum of heavy rare earth elements (ΣHREE), as well as the decrease in concentrations of niobium (Nb), strontium (Sr), and titanium (Ti) in the rocks under investigation, can be attributed to processes occurring in the mid-upper crust or the production of their parent rocks through subduction-related mechanisms [6, 354]. A similar pattern was also observed in the MSB granite over the time period of approximately 1800 to 1700 Ma.

Table 6.1 Whole-rock geochemistry data for mafic granulites of Betul Belt.

Sample	BG-2	BG-5	BG-9	N-4	N-7A	N-14	N-16	N-17B	CH-3	CH-04	CH-06	CH-12
SiO_2	47.51	48.83	48.19	48.93	46.82	48.27	49.57	48.63	51.18	48.89	46.76	52.66
Al_2O_3	14.27	15.23	15.31	15.24	13.97	15.16	14.26	13.97	15.07	14.65	13.43	14.21
CaO	7.96	8.29	7.57	8.83	9.87	8.14	7.95	9.26	1.04	1.13	0.99	0.71
Fe_2O_3	16.97	14.28	13.93	14.75	13.65	17.25	16.41	17.89	13.54	14.37	14.60	12.92
K_2O	0.76	0.84	0.81	1.29	0.66	0.86	0.68	0.79	0.17	0.18	0.18	0.18
MgO	7.58	8.63	9.06	4.81	12.08	4.91	7.49	5.00	5.37	6.30	7.41	4.68
MnO	0.24	0.55	1.57	0.22	0.21	0.68	0.70	0.58	8.22	8.50	7.64	7.99
Na_2O	2.14	2.52	1.98	2.54	1.99	2.18	2.47	2.37	2.11	2.15	1.93	2.05
P_2O_5	0.32	0.10	0.48	0.48	0.55	0.08	0.08	0.05	0.58	0.51	0.49	0.45
TiO_2	1.26	1.29	1.71	1.00	0.74	0.14	0.14	0.58	0.56	0.53	0.45	0.41
LOI	1.10	0.56	0.64	1.81	0.54	1.33	0.24	0.88	1.16	1.80	4.11	3.73
Total	99.00	100.55	100.61	98.09	100.54	97.67	99.76	99.12	97.84	97.20	93.89	96.27
Sc	19.47	25.79	53.63	31.22	31.40	2.89	8.32	19.19	34.19	34.74	36.87	33.09
V	207.27	163.17	113.01	188.09	171.44	23.08	42.69	183.75	268.92	247.05	280.36	216.18
Co	37.62	30.14	19.87	32.60	57.11	21.92	11.47	40.12	41.17	35.99	44.47	38.78
Ni	29.95	69.89	18.06	51.48	438.44	98.36	24.66	61.66	46.08	39.43	49.83	43.94
Cu	30.80	28.68	37.85	56.25	34.22	871.68	93.92	430.95	92.74	75.11	91.95	93.46
As	4.69	2.94	3.46	4.88	5.15	4.51	3.14	3.36	6.19	10.54	10.46	7.84
Rb	1.52	1.97	2.98	34.35	18.34	0.99	1.93	21.69	8.16	8.19	10.42	6.65
Sr	8.58	3.47	6.52	237.99	142.31	27.45	14.85	173.63	335.46	369.51	321.84	347.99
Y	12.93	18.39	57.43	40.39	31.75	11.49	22.02	21.23	37.95	31.72	33.69	29.50
Zr	118.16	133.85	84.40	165.28	231.88	31.74	66.52	84.89	40.57	64.46	56.96	71.02
Nb	9.98	10.27	10.83	14.32	6.69	4.43	7.20	6.66	10.52	10.61	10.43	9.22
Mo	0.61	1.14	9.49	1.56	0.74	2.17	3.21	1.75	2.93	1.85	1.61	1.48
Cd	0.24	0.32	0.59	0.16	0.33	0.72	0.31	0.34	0.25	0.22	0.27	0.26
Cs	0.46	0.32	0.14	2.04	1.72	0.21	0.29	0.71	0.92	1.08	1.12	0.92
Ba	51.17	91.41	145.71	671.59	340.81	387.83	242.25	784.73	780.91	782.60	968.04	586.06
Hf	2.65	3.13	2.06	3.74	4.77	0.70	1.64	2.02	1.33	1.80	1.92	2.04
Pb	1.09	1.05	2.73	15.41	9.58	3.25	1.91	7.67	10.26	9.24	17.33	8.29
Th	6.21	4.19	2.77	2.94	3.73	6.43	3.65	6.29	0.40	1.47	1.94	2.05
U	0.92	0.90	0.57	1.38	0.51	2.12	0.36	0.65	0.17	0.20	0.40	0.46
La	101.11	80.83	117.03	147.84	120.22	81.04	145.70	151.72	36.27	29.25	32.03	29.13
Ce	213.99	170.31	218.06	279.04	228.79	154.69	277.51	291.03	86.13	63.46	72.10	62.97
Pr	21.77	19.05	21.61	32.54	26.53	17.88	31.95	31.57	10.76	7.55	8.54	7.60
Nd	79.01	72.06	73.21	121.05	97.85	67.80	118.44	110.67	43.45	30.70	34.21	30.92
Sm	14.31	13.28	11.14	22.42	18.53	12.07	22.06	16.43	8.66	5.99	6.76	6.18
Eu	2.77	2.47	2.11	4.22	3.68	2.49	4.40	1.31	1.84	1.52	1.77	1.41
Gd	13.28	10.98	9.81	21.08	17.14	11.57	20.79	12.45	9.19	6.19	6.81	6.34
Tb	1.92	1.50	1.24	2.86	2.52	1.72	2.99	1.39	1.26	0.85	0.93	0.86
Dy	11.46	7.82	6.93	16.93	14.57	9.80	17.62	6.44	7.14	5.16	5.53	5.28
Ho	2.33	1.48	1.30	3.15	2.73	1.95	3.35	1.15	1.44	1.02	1.11	1.03
Er	6.69	4.12	3.62	9.02	7.41	5.24	9.05	3.18	3.91	2.97	3.16	3.04
Tm	1.07	0.58	0.53	1.22	1.07	0.75	1.24	0.40	0.58	0.42	0.45	0.41
Yb	6.80	3.87	3.80	7.51	6.61	4.84	8.43	2.87	3.66	2.89	3.00	2.82
Lu	1.02	0.53	0.50	1.13	1.02	0.72	1.15	0.43	0.57	0.41	0.44	0.43
ΣREE	477.54	388.88	470.89	669.99	548.67	372.55	664.66	631.06	215.44	160.05	179.20	160.93
La_N/Lu_N	10.68	16.47	25.18	14.01	12.67	12.06	13.58	38.05	6.86	7.60	7.82	7.23

Table 6.2 Whole-rock geochemistry data for Pelitic granulites of Betul Belt

Sample	BK-3	BK-6	BK-7	BK-9	SG-3	SG-5	SG-7
SiO_2	60.80	63.12	65.25	63.89	62.45	60.82	65.49
Al_2O_3	16.87	18.21	15.37	15.26	12.49	15.27	11.23
CaO	1.99	0.36	1.58	2.27	5.25	4.23	4.99
Fe_2O_3	9.28	7.54	6.39	7.64	7.74	7.25	8.42
K_2O	4.05	2.91	4.89	5.49	4.34	3.69	2.16
MgO	1.89	1.21	0.81	2.28	1.63	1.85	1.96
MnO	0.82	0.07	0.18	0.19	0.03	0.06	0.02
Na_2O	1.98	2.59	2.67	0.45	2.16	3.89	2.69
P_2O_5	0.02	0.01	0.00	0.01	0.05	0.04	0.03
TiO_2	0.15	0.24	0.18	0.20	0.94	0.60	1.22
LOI	1.15	3.74	2.76	2.32	2.82	2.30	1.80
Total	97.85	96.26	97.34	97.68	97.08	97.70	98.20
Sc	5.63	7.31	5.17	5.79	7.39	6.25	7.57
V	24.55	18.35	29.77	33.19	32.40	38.66	36.88
Co	1.97	1.61	1.99	2.64	15.81	10.57	4.35
Ni	18.36	10.02	11.64	31.31	38.32	31.32	19.35
Cu	9.13	9.03	19.35	17.80	32.35	43.37	20.02
As	28.83	5.83	6.47	9.31	24.29	17.84	9.81
Rb	107.91	77.73	49.09	55.89	31.75	12.39	59.03
Sr	19.51	14.64	10.21	11.67	9.83	11.44	17.66
Y	39.27	40.39	57.47	58.28	14.54	10.80	61.50
Zr	541.07	848.60	684.68	728.74	1162.96	719.87	1138.73
Nb	15.19	16.04	12.27	12.98	14.04	8.36	19.26
Mo	1.04	1.43	0.85	1.05	2.15	2.21	1.40
Cd	0.67	0.12	0.20	0.19	0.21	0.14	0.25
Cs	1.17	0.23	0.23	0.30	3.63	7.57	1.62
Ba	884.06	859.91	1192.58	1298.80	367.04	323.74	367.48
Hf	11.14	17.64	13.86	14.96	25.49	15.44	24.39
Pb	4.41	4.66	4.77	5.56	11.32	5.84	9.39
Th	33.49	33.69	28.89	23.23	32.82	43.44	44.78
U	8.36	7.83	7.75	4.68	8.23	9.57	12.07
La	91.65	88.17	79.55	54.84	88.36	128.77	134.58
Ce	164.43	172.02	162.77	93.69	184.30	250.71	263.96
Pr	18.50	18.74	17.86	9.81	19.27	28.09	29.46
Nd	63.40	67.39	65.95	34.65	70.46	104.80	109.27
Sm	10.96	12.65	12.58	6.72	11.95	19.79	20.67
Eu	2.07	2.20	2.39	1.39	2.12	3.79	4.13
Gd	9.25	10.35	10.68	6.70	9.49	17.38	18.56
Tb	1.24	1.47	1.45	0.94	1.22	2.47	2.60
Dy	7.78	8.93	8.49	5.66	6.97	14.14	15.24
Ho	1.48	1.72	1.59	1.16	1.32	2.71	2.91
Er	4.35	4.85	4.83	3.59	3.75	7.61	8.10
Tm	0.67	0.74	0.68	0.53	0.60	1.07	1.08
Yb	4.24	5.47	4.83	3.52	3.78	6.37	6.97
Lu	0.61	0.70	0.70	0.54	0.55	0.98	0.96
ΣREE	380.62	395.41	374.34	223.74	404.16	588.70	618.49
La_N/Lu_N	16.10	13.48	12.22	10.90	17.22	14.05	14.99